Acta Cryst. (1993). D**49**, 534–540

High-Resolution Structure of the Complex Between Carboxypeptidase A and L-Phenyl Lactate

BY ALEXEI TEPLYAKOV AND KEITH S. WILSON

EMBL, c/o DESY, Notkestrasse 85, 2000 *Hamburg* 52, *Germany*

PIERLUIGI ORIOLI

Dipartimento di Chimica, Universita di Firenze, Via Gino Capponi 7, 50121 *Firenze, Italy*

AND STEFANO MANGANI

Dipartimento di Chimica, Universita di Siena, Pian dei Mantellini 44, 53100 *Siena, Italy*

(*Received* 14 *April* 1993; *accepted* 8 *July* 1993)

Abstract

The X-ray structures of native carboxypeptidase A and of the enzyme–inhibitor complex with L-phenyl lactate have been refined at 1.54 and 1.45 Å resolution to *R* factors of 0.151 and 0.161, respectively. Crystals of the complex were isomorphous with the native crystals (space group $P2_1$, $a = 51.60$, $b = 60.27$, $c = 47.25$ Å, $\beta = 97.27°$). The high-resolution electron density allowed correction of many side-chain positions in the classical carboxypeptidase A model. This reflects the advantages of the high-quality complete synchrotron data collected with an imaging plate detector. The conformational changes in the active centre of the enzyme upon binding of the inhibitor are restricted to only two residues, Tyr248 and Arg145. L-Phenyl lactate is bound in the S1′ pocket and forms hydrogen bonds to Arg145, Glu270 and to the zinc-bound water molecule. The present structure provides an explanation for the higher stability of the complexes with the products of esterolysis in comparison with those of amidolysis. This is consistent with the finding that product release is rate limiting for esters but not for peptides.

Introduction

Carboxypeptidase A (CPA, E.C. 3.4.17.1) is a zinc exopeptidase which specifically catalyzes hydrolysis of C-terminal peptide and ester substrates showing preference towards residues with aromatic side chains (Hartsuck & Lipscomb, 1971; Auld & Vallee, 1987; Christianson & Lipscomb, 1989). The C-terminal products of hydrolysis, *i.e.* simple aromatic amino acids or their alcohol analogues, are inhibitors of CPA (Bicknell *et al.*, 1988). L-Phenyl lactate (L-OPhe) is one of the products of CPA ester hydrolysis. Its affinity for the enzyme can be estimated from the inhibition constant $K_i = 1.3 \times 10^{-4}$ *M* (Byers & Wolfenden, 1973). It compares well with the apparent dissociation constant of the complex estimated spectroscopically in cobalt-substituted CPA: $K_d = 5 \times 10^{-4}$ *M* (Bicknell *et al.*, 1988). These values indicate that L-OPhe binds to CPA about 40 times tighter than its amino-acid homologue L-Phe ($K_i = 55 \times 10^{-4}$ *M*) (Byers & Wolfenden, 1973).

Although in principle peptide and ester hydrolysis can follow different reaction pathways, evidence has been provided that both follow the same scheme in CPA:

$$E + S \Longleftrightarrow ES_1 \Longleftrightarrow ES_2 \Longleftrightarrow E + P$$

and that both peptides and esters bind to the active site prior to the rate-limiting step (Auld *et al.*, 1984; Geoghegan, Galdes, Martinelli, Auld & Vallee, 1983; Geoghegan *et al.*, 1986; Galdes, Auld & Vallee, 1986). These cryokinetic studies demonstrate that hydrolysis of esters occurs prior to the rate-limiting step so that the intermediate ES_2 can be more correctly described as a ternary complex EP_1P_2 where P_1 and P_2 are products of esterolysis or substrates for the reverse reaction. In contrast, peptide hydrolysis is either simultaneous or follows the rate-limiting step. It was proposed that the release of the products from the active site is rate limiting for esterolysis, whereas in peptide hydrolysis the rate-limiting step is hydrolysis of the amide bond (Auld *et al.*, 1984). On the basis of crystallographic studies, Christianson & Lipscomb (1989) suggested that, in spite of the different intermediates observed, the modes by which peptides and esters bind to the enzyme can be distinguished by the different roles played by zinc and Arg127.

The peptide hydrolysis product L-Phe has been observed in the structures of ternary complexes with a hydrolyzed phosphonamidate inhibitor (Christian-

ISSN 0907-4449

son & Lipscomb, 1986), an enzyme–substrate–product complex (Christianson & Lipscomb, 1987) and in the complex with azide anion (Mangani & Orioli, 1992). In the former structure, however, L-Phe is probably bound in a non-productive mode because of interactions with the phosphonate (Christianson & Lipscomb, 1986). The present study aims to discover whether the higher affinity of L-OPhe for CPA is as a result of differences in the binding mode with respect to L-Phe or is simply due to the different electronic properties of the amide and hydroxyl groups. Furthermore, the structure of the L-OPhe complex can help to rationalize the observed differences in the mechanism of ester and peptide hyrolysis by CPA.

We have determined the crystal structure of the CPA–L-OPhe complex at 1.45 Å resolution using the atomic model of native CPA (Rees, Lewis & Lipscomb, 1983) for difference Fourier map calculations. Surprisingly many side chains have been found in different orientations in these two structures. To be certain that the observed differences between the complex and the native structure do not reflect real changes, we have also collected native CPA data to 1.54 Å resolution and refined the model using these data.

Experimental procedure

Crystallization and X-ray data collection

Crystals of CPA were prepared as described by Lipscomb *et al.* (1966), cross linked with glutaraldehyde and soaked in 20 m*M* HEPES buffer solution at pH 7.5, containing 35 m*M* L-OPhe for 1 week at 277 K. Crystals of the complex were isomorphous to the native crystals. They belong to the space group $P2_1$, with unit-cell parameters $a = 51.60\ (5)$, $b = 60.27\ (20)$, $c = 47.25\ (16)$ Å and $\beta = 97.27\ (2)^\circ$.

X-ray data were collected on EMBL synchrotron beamline X31 at a wavelength of 0.92 Å using an imaging-plate detector (J. Hendrix & A. Lentfer, unpublished results). A single protein crystal of approximate size 0.5 × 0.5 × 0.5 mm was used for each data set. Complete 90° rotation around crystallographic axis *a* was repeated twice for each crystal with shorter exposures in order to measure intensities of strong reflections. The maximum resolution of the data was 1.54 Å for the native crystal and 1.45 Å for the crystal of the complex. No absorption correction was applied as absorption was negligible at the short wavelength. Statistics of the X-ray experiments are given in Table 1.

Crystal structure determination

The atomic model of CPA from the Protein Data Bank (5CPA; Bernstein *et al.*, 1977) was refined by Rees, Lewis & Lipscomb (1983) to $R = 0.190$ at 1.54 Å resolution using the restrained least-squares procedure of Hendrickson & Konnert (1981). It was used for the structure determination of CPA and CPA–L-OPhe. The model was refined using the *CCP*4 (SERC Daresbury Laboratory, 1979) version of the program *PROLSQ* (Hendrickson & Konnert, 1981), first with the CPA–L-OPhe data. Manual correction of the model was carried out using an Evans & Sutherland PS300 graphics system with the program *FRODO* (Jones, 1978). L-OPhe and water molecules were included in the model on the basis of difference electron-density maps. No contact restraints were applied to the water molecules and the zinc ion. Occupancies of the water molecules were set to unity and not refined. Water molecules with temperature factors greater than 50 Å^2 were excluded from the model. The atomic model of CPA–L-OPhe was used for refinement of the native CPA using the same protocol as described for CPA–L-OPhe.*

Table 1. *Statistics of the X-ray experiments*

	CPA	CPA–L-OPhe
Wavelength (Å)	0.92	0.92
High resolution		
Maximum resolution (Å)	1.54	1.45
Oscillation angle per exposure ( )	1.25	1.25
Total oscillation range ( )	90	90
Medium resolution		
Maximum resolution (Å)	2.5	2.5
Oscillation angle per exposure ( )	2.5	2.5
Total oscillation range ( )	90	90
Low resolution		
Maximum resolution (Å)	3.5	3.5
Oscillation angle per exposure ( )	3.0	3.0
Total oscillation range ( )	90	90
Number of measured reflections	91192	127939
Number of unique reflections	37803	46136
$R_{merge} = \sum \langle I \rangle - I_i / \sum I_i$ (%)	4.3	3.6
Completeness (%)	88.7	90.4
Highest resolution completeness* (%)	90.3	78.8

* The highest resolution shell contains 1000 theoretically predicted reflections.

Results and discussion

Crystal structure of native CPA

The crystal structure of native CPA has been refined to a crystallographic R factor ($R = \sum |F_o - F_c| / \sum F_o$, where F_o and F_c are the observed and calculated structure amplitudes, respectively) of 0.151 for all 37 638 observed reflections in the resolution range 8.0–1.54 Å. The model contains 2437 protein atoms

* Atomic coordinates and structure factors of native CPA (Reference: 1CTB, R1CTBSF) and the CPA–L-OPhe complex (Reference: 1CTC, R1CTCSF) have been deposited with the Protein Data Bank, Brookhaven National Laboratory. Free copies may be obtained through The Technical Editor, International Union of Crystallography, 5 Abbey Square, Chester CH1 2HU, England (Supplementary Publication No. SUP 37095). A list of deposited data is given at the end of this issue.

(all 307 residues), one zinc ion and 218 water molecules. Stereochemical parameters of the model are presented in Table 2. The overall coordinate error in atomic positions estimated from the σ_A plot (Read, 1986) is 0.10 Å.

The mean temperature factor (B factor) calculated for all protein atoms is 14.3 Å^2. B factors averaged over the main-chain atoms are plotted as a function of residue number in Fig. 1. Beside the N and C termini of the chain, there are only two regions with B factors significantly higher than the mean value: residues 57–58 and 133–135. The electron density for these residues is very weak and the tracing of the peptide chain is ambiguous. They were modelled so that the conformational angles φ and ψ would fall within the allowed regions in the Ramachandran plot (Fig. 2). In this respect they differ from the 5CPA model. There are three residues with unfavourable φ/ψ combinations in the present CPA structure. The electron density is very clear for each of them. The abnormal conformations of Ser199 and Asp273 are related to the *cis*-peptide bonds before Phe198 and Asp273 which are probably required for the correct folding of the protein. Ile247 can easily change its conformation following the large movement of Tyr248 caused by substrate binding (see below). The electron density indicated static disorder for the side chains of Ser194, Ser199 and Gln261 which were refined in two alternative positions each with relative occupancies of 0.5.

Comparison of the refined native CPA structure with the 5CPA model shows a surprising number of deviations as a result of different conformations of amino-acid side chains. In total there are 48 residues (22 of which are internal) which deviate by more than 60° in side-chain torsion angles (Table 3). Most of these residues contain branched side chains with chiral atoms (Fig. 3). Their torsion angles in the present model have energetically favourable values around ±60 and 180°. The high-resolution electron density which allowed correction of the classical CPA model, reflects the advantages of the high quality synchrotron data available with an imaging-plate detector. Data used for refinement of the 5CPA model were collected with a diffractometer on a Cu $K\alpha$ X-ray source and contained 32 080 reflections to 1.54 Å resolution (75% complete). As the protein itself and the crystals appear to be identical in the two studies, the quality of the X-ray data is probably the only reason for the improved electron-density maps.

Water molecules in the CPA structure were selected from the $(F_o - F_c)$ maps as peaks with a height of at least 3σ with the help of the program *PEAKMAX* of the *CCP*4 suite (SERC Daresbury Laboratory, 1979). The final CPA model contains 218 water molecules, 200 of which form direct hydro-

Table 2. *Refinement statistics*

Parameter	Target σ*	CPA	CPA L-OPhe	5CPA†
Bond distances (Å)				
1–2 neighbours	0.020	0.014	0.014	0.024
1–3 neighbours	0.040	0.035	0.037	0.041
1–4 neighbours	0.050	0.044	0.054	0.047
Planar groups (Å)	0.020	0.013	0.013	0.038
Chiral volumes (Å^3)	0.150	0.140	0.137	0.263
Single torsion contacts (Å)	0.300	0.133	0.138	0.191
Multiple torsion contacts (Å)	0.300	0.163	0.163	0.468
Torsion angles ( )				
Planar (peptide)	3.0	2.5	2.5	8.5
Staggered (aliphatic)	15.0	14.3	15.0	18.6
Orthonormal (aromatic)	20.0	28.4	28.8	
Temperature factors (Å^2)				
Main chain	4.0	3.0	2.6	4.5
Side chain	6.0	6.7	5.5	7.5

* The target σ is the inverse square root of the least-squares weight used for refinement of CPA and CPA L-OPhe.

† Parameters for the 5CPA model were taken from Rees, Lewis & Lipscomb (1983).

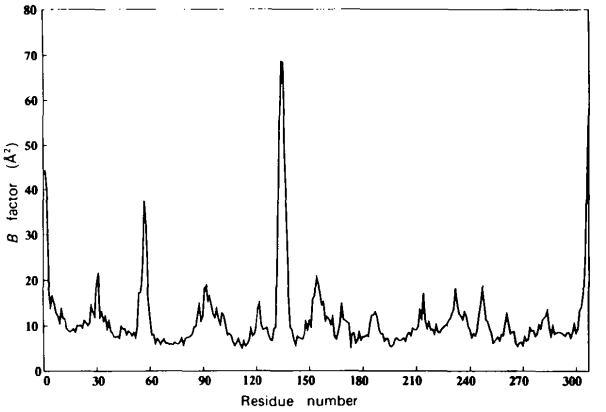

Fig. 1. The average main-chain B factors as a function of residue number for the native CPA model.

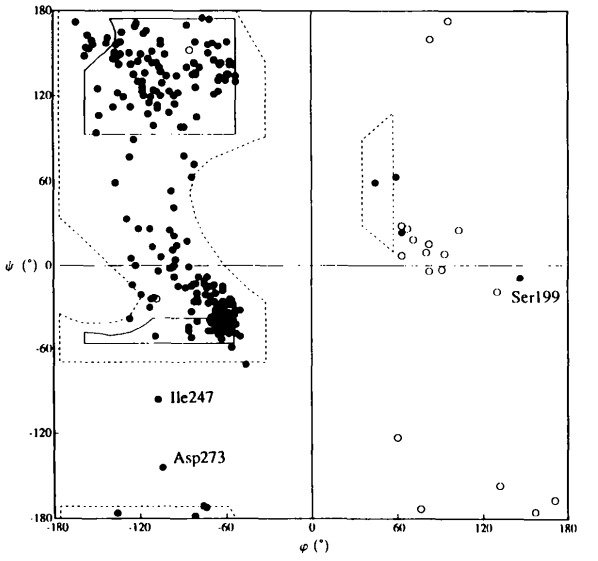

Fig. 2. The φ/ψ plot for the native CPA model.

gen bonds with protein atoms. 22 water molecules are buried in the protein, *i.e.* have accessible surface of less than 0.5 Å^2 as estimated with the program *ACCESS* (SERC Daresbury Laboratory, 1979) using a probe radius of 1.4 Å. All but one of the internal waters are present in the 5CPA model. The water structure in the active-site pocket is very similar in the two models. In addition to eleven molecules in the 5CPA structure, six new positions were identified which might be the consequence of phase improvement or higher completeness of the X-ray data. The quality of the data seems to be crucial for positional refinement of the water structure. Although no contact restraints were applied, all water molecules in the present CPA structure lie within 2.4–3.4 Å of hydrogen-bond donors/acceptors. There are 36 molecules outside these limits in the 5CPA structure, five of them at distances less than 1 Å from other atoms.

Differences between the two CPA models are restricted to fine details of the protein and water structures which are the most sensitive to the high-resolution data. This is reflected by the crystallographic R factor plotted as a function of resolution in Fig. 4. At high resolution the R factor goes up to 28% for 5CPA as compared to $R = 20\%$ for the present structure.

*Crystal structure of the complex CPA–*L-*OPhe*

The crystal structure of the complex CPA–L-OPhe has been refined to an R factor of 0.161 for all 45 829 observed reflections in the resolution range

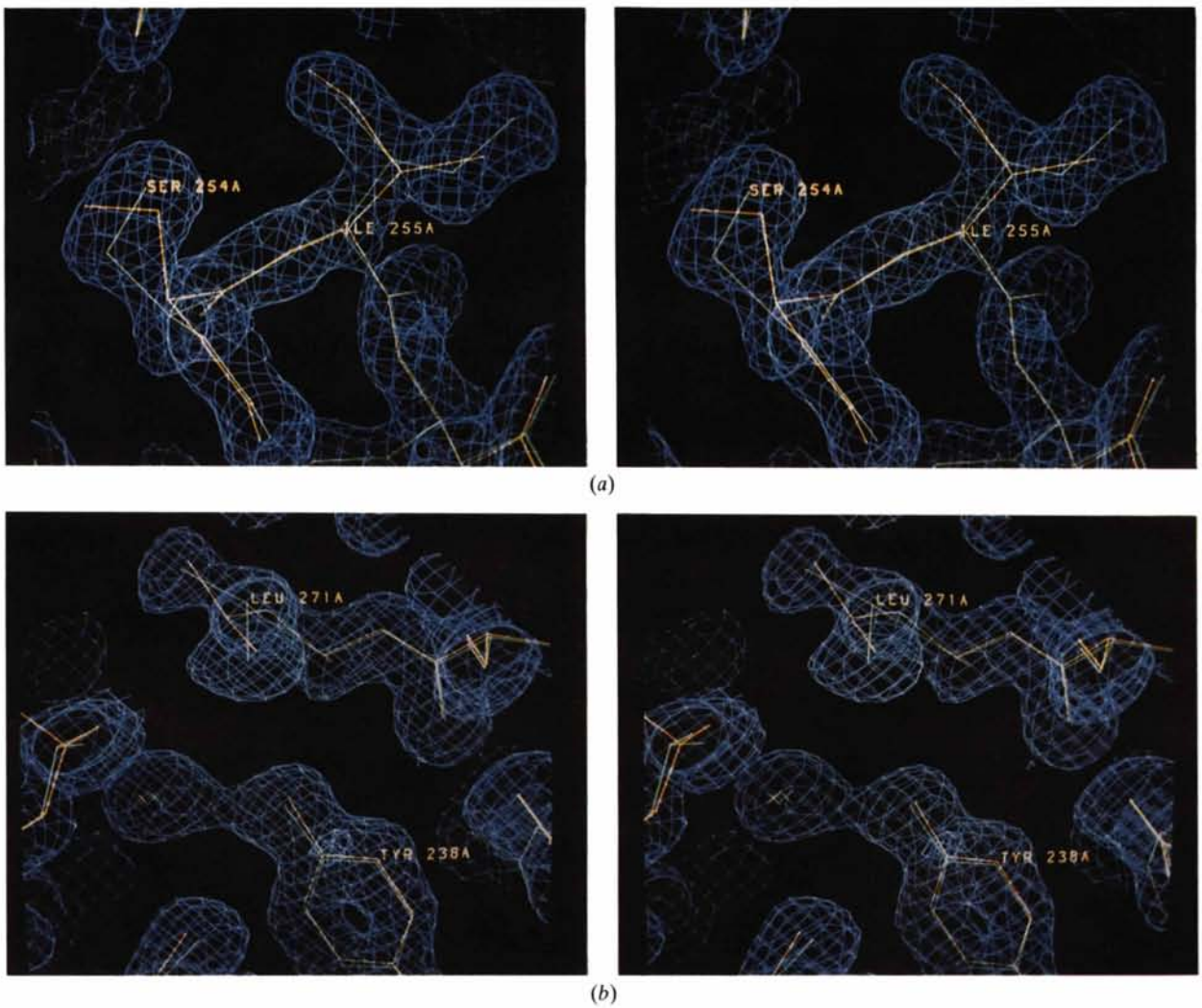

Fig. 3. Representative fragment of the $(3F_o - 2F_c)$ electron density of CPA contoured at the level of 1.5σ, where σ is the root-mean-square deviation. The present CPA model is shown in green, the 5CPA model is shown in orange. (*a*) Ser254 and Ile255; (*b*) Leu271 and Tyr238 with the hydrogen-bonded water molecule.

8.0–1.45 Å. The model contains 2437 protein atoms, 12 atoms of L-OPhe, one zinc ion and 181 water molecules. Refinement statistics are given in Table 2.

The electron density clearly shows the position of the L-OPhe molecule in the S1′ pocket and the phenyl ring of Tyr248 in the 'down' conformation, *i.e.* bound to the L-OPhe carboxylate (Fig. 5). The refined atomic *B* factors for L-OPhe vary from 13.0 to 21.6 Å^2 and are only slightly higher than the mean *B* factor of the protein molecule (16.5 Å^2). This indicates that the occupancy of L-OPhe in the crystal complex is close to 100%.

Compared to the native structure, only two residues change their conformation upon binding of the inhibitor. Ile247 undergoes slight reorientation following the large movement of Tyr248 from the 'up' to the 'down' position. Arg145 switches from the 'free' state to the 'bound' state when it forms hydrogen bonds to the L-OPhe carboxylate and to the main-chain carbonyl of Asn144 and loses its hydrogen bond to Asp142. Such rearrangement of the hydrogen-bonding network has also been observed upon binding of phosphonate inhibitors to CPA (Kim & Lipscomb, 1991). The side chain of Arg145 is rather flexible in the 'free' state as can be judged from the high atomic *B* factors which are 5–6 times higher than the main-chain *B* factors in both the present native CPA structure and the 5CPA model. The salt bridge to the carboxyl of Asp142 is thought to play a stabilizing role in the absence of a substrate.

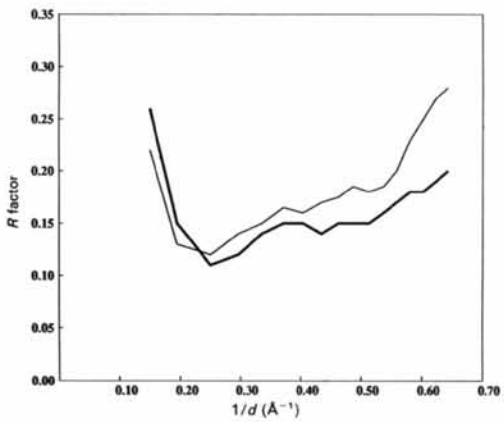

Fig. 4. Dependence of the crystallographic *R* factor on the resolution for the present CPA (thick line) and 5CPA (Rees, Lewis & Lipscomb, 1983; thin line) structures.

The mode of binding of L-OPhe observed in the present crystal structure is similar to that found for L-Phe in the ternary complex CPA–L-Phe–azide (Mangani & Orioli, 1992) but differs from that observed for L-Phe in the structure of an enzyme–substrate–product complex with *N*-benzoyl-L-phenylalanine (Christianson & Lipscomb, 1987). The carboxylate of L-OPhe is salt linked to Arg145 and also receives hydrogen bonds from Asn144 and Tyr248 (Table 4). The L-OPhe phenyl ring occupies the hydrophobic S1′ pocket formed by residues Leu203, Ile243, Ile247, Ala250, Gly253, Ile255 and Thr268, and covered by Tyr248. The difference lies in the orientation of the L-Phe amino group which is not hydrogen bonded to Glu270 in the latter structure. In the present structure the hydroxyl group of L-OPhe forms hydrogen bonds with the Glu270 carboxylate (2.4 Å) and with the zinc-bound water molecule (2.7 Å) which reinforces binding of the inhibitor. An amino group (both in the neutral and in the protonated form) certainly cannot perform two such interactions acting at the same time as a

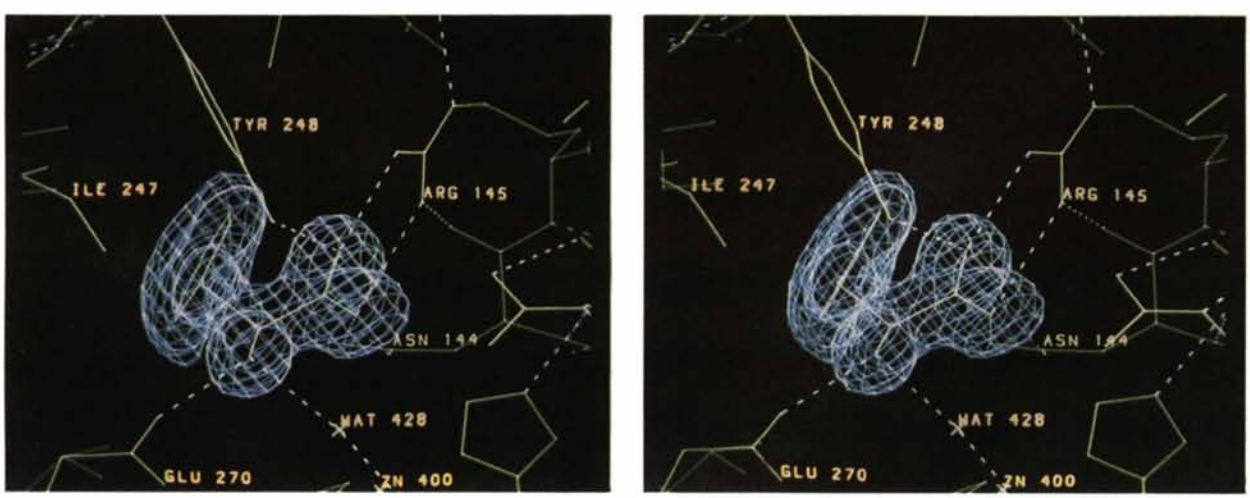

Fig. 5. Stereoview of the $(F_o - F_c)$ electron density in the active centre of the CPA–L-OPhe structure. L-OPhe atoms were omitted from the phase calculation. Electron density contours are at the 3σ level above the mean value. Hydrogen bonds are shown in dashed lines.

Table 3. *Comparison of the native CPA models*

Residue	Acc.* (Å²)	Torsion angles (°) in 5CPA†					Torsion angles (°) in 1CTB‡				
		χ_1	χ_2	χ_3	χ_4	χ_5	χ_1	χ_2	χ_3	χ_4	χ_5
Arg2	234	−96.2	−167.7	−90.7	−172.1	17.5	61.0	−151.0	36.4	173.2	−0.1
Thr6	88	−100.7	–	–	–	–	62.0	–	–	–	–
Leu15	17	−166.1	−78.6	–	–	–	170.7	60.2	–	–	–
Asp16	116	−47.3	82.6	–	–	–	−70.1	−32.4	–	–	–
Met22	1	−57.8	178.2	116.6	–	–	−60.3	−178.8	−179.7	–	–
Glu31	176	−103.9	65.1	60.3	–	–	−57.5	−49.4	−63.4	–	–
Val33	2	25.9	–	–	–	–	163.0	–	–	–	–
Ser34	52	−57.4	–	–	–	–	47.2	–	–	–	–
Ser57	114	−59.0	–		–		179.4	–	–	–	–
Asn58	91	146.3	103.6		–	–	−120.3	103.3	–		–
Ile62	0	−43.4	−58.6	–	–	–	−65.8	141.8	–	–	–
Gln92	148	−52.0	−54.8	123.3	–	–	−71.9	−167.1	28.0	–	
Thr97	24	142.1	–		–	–	−54.2	–	–	–	–
Leu100	0	−97.3	−176.2	–		–	−145.7	52.7	–	–	–
Glu122	135	−88.4	8.1	−65.6		–	−54.5	−68.1	−34.5	–	–
Arg127	26	63.7	128.4	63.1	173.6	−41.6	71.4	−160.8	−57.4	−93.7	−0.1
Val132	96	−68.6	–	–	–	–	155.3	–	–	–	–
Ser134	105	142.0	–	–	–	–	67.5		–	–	
Leu137	178	−19.7	−56.6	–	–	–	−90.3	−143.3	–	–	–
Val139	31	9.0	–	–	–	–	174.1	–	–	–	–
Lys153	109	−66.1	−167.4	169.4	−88.7	–	−64.0	−167.6	−175.4	165.4	
Lys168	155	22.0	165.6	−163.8	160.5	–	174.9	−165.5	111.8	161.4	–
Ile179	0	−55.9	31.0	–	–	–	−59.8	175.3	–	–	–
Lys184	103	−67.4	−175.4	26.3	−157.6	–	−76.8	−163.3	−151.0	139.2	–
Leu193	0	−91.4	41.5		–	–	−49.5	−169.6	–	–	–
Leu202	0	−144.0	−156.3	–	–	–	174.2	57.0	–	–	–
Leu203	3	−88.7	2.9		–	–	44.3	163.8		–	–
Lys216	97	−169.1	−106.1	−109.8	51.0		−176.8	−170.8	179.0	−141.6	
Leu219	0	−93.8	43.8	–	–	–	−61.2	−151.9	–	–	–
Val227	17	159.6	–	–	–	–	−52.1	–	–	–	–
Lys231	108	−178.5	−177.8	173.1	102.4		171.4	168.1	56.2	157.0	–
Leu233	78	−100.5	−158.2	–	–	–	−143.7	58.6	–	–	–
Lys239	130	−91.2	82.8	101.5	−25.1	–	−56.7	155.2	−85.5	177.2	–
Thr245	112	−101.0	–	–		–	65.6	–	–	–	–
Thr246	46	93.1	–		–	–	−50.8	–	–		–
Gln249	58	−148.9	−169.4	138.5		–	−167.8	161.6	39.5	–	–
Ser254	2	−130.3	–		–	–	72.8		–	–	–
Ile255	3	−80.5	−43.8	–		–	69.9	162.1		–	
Lys264	54	−178.1	176.0	−40.2	171.8	–	179.1	175.1	163.7	−167.	
Thr268	10	−39.7	–	–	–	–	174.1	–	–	–	–
Leu271	0	−89.1	27.7		–	–	−49.1	−177.3	–	–	–
Arg276	206	−150.9	−71.5	119.1	159.1	51.8	−179.0	159.8	169.9	−152.0	0.4
Leu280	94	−102.4	60.6	–	–	–	46.2	−175.6	–	–	–
Leu281	5	−137.1	−118.6		–		164.1	80.0	–		–
Ile287	53	−75.9	−29.4	–	–	–	−71.0	166.4	–	–	–
Thr293	0	178.1	–		–	–	−53.1	–	–	–	–
Leu295	49	96.3	40.1	–	–	–	−54.9	178.2		–	–
Leu298	16	−150.5	−140.4	–	–		177.3	57.2	–	–	

* Accessible surface calculated with the program *DSSP* (Kabsch & Sander, 1983).
† The 5CPA model of Rees, Lewis & Lipscomb (1983).
‡ The present native CPA structure.

Table 4. *Enzyme–inhibitor interactions in the CPA–L-OPhe complex*

CPA atom	L-OPhe atom	Distance (Å)
Glu270 O*E*2	Hydroxyl O	2.38
Zn-bound water	Hydroxyl O	2.72
Tyr248 OH	Carboxylate O1	2.65
Arg145 NH2	Carboxylate O1	2.61
Arg127 NH2	Carboxylate O1	3.38
Arg145 NH1	Carboxylate O2	2.97
Asn144 N*D*2	Carboxylate O2	2.86

hydrogen-bond donor towards Glu270 and an acceptor towards the zinc-bound water molecule.

This structural observation may explain the higher stability of the CPA–L-OPhe complex with respect to the CPA–L-Phe complex. If we consider it from a mechanistic point of view, then the present structure can provide a very simple explanation for the differences between peptide and ester hydrolysis (Galdes, Auld & Vallee, 1986). When the product P_2 is released from the EP_1P_2 complex upon coordination of a water molecule to the zinc ion, the product complex EP_1 is stabilized by a hydrogen bond to the water only in the case of the ester hydrolysis product L-OPhe. The peptide hydrolysis product L-Phe does not have this extra stabilization and consequently is more readily displaced by the substrate. This mechanism is consistent with previous findings (Galdes, Auld & Vallee, 1986) and may explain why the product release is rate limiting for esters but not for peptides.

References

AULD, D. S., GALDES, A., GEOGHEGAN, K. F., HOLMQUIST, B., MARTINELLI, R. A. & VALLEE, B. L. (1984). *Proc. Natl Acad. Sci. USA.* **82**, 5041–5045.

AULD, D. S. & VALLEE, B. L. (1987). *Hydrolytic Enzymes*, edited by A. NEUBERGER & K. BROCKLEHURST, pp. 201–255. Amsterdam: Elsevier.

BERNSTEIN, F. C., KOETZLE, T. F., WILLIAMS, G. J. B., MEYER, E. F. JR, BRICE, M. D., ROGERS, J. R., KENNARD, O., SHIMANOUCHI, T. & TASUMI, M. (1977). *J. Mol. Biol.* **122**, 535–542.

BICKNELL, R., SCHÄFFER, A., BERTINI, I., LUCHINAT, C., VALLEE, B. L. & AULD, D. S. (1988). *Biochemistry*, **27**, 1050–1057.

BYERS, L. D. & WOLFENDEN, R. (1973). *Biochemistry*, **12**, 2070–2078.

CHRISTIANSON, D. W. & LIPSCOMB, W. N. (1986). *J. Am. Chem. Soc.* **108**, 545–546.

CHRISTIANSON, D. W. & LIPSCOMB, W. N. (1987). *J. Am. Chem. Soc.* **109**, 5536–5538.

CHRISTIANSON, D. W. & LIPSCOMB, W. N. (1989). *Acc. Chem. Res.* **22**, 62–69.

GALDES, A., AULD, D. S. & VALLEE, B. L. (1986). *Biochemistry*, **25**, 646–651.

GEOGHEGAN, K. F., GALDES, A., HANSON, G., HOLMQUIST, B., AULD, D. S. & VALLEE, B. L. (1986). *Biochemistry*, **25**, 4669–4674.

GEOGHEGAN, K. F., GALDES, A., MARTINELLI, R. A., AULD, D. S. & VALLEE, B. L. (1983). *Biochemistry*, **22**, 2255–2262.

HARTSUCK, J. A. & LIPSCOMB, W. N. (1971). *The Enzymes*, 3rd ed., Vol. 3, edited by P. D. BOYER, pp. 1–56. New York: Academic Press.

HENDRICKSON, W. A. & KONNERT, J. H. (1981). *Biomolecular Structure, Conformation, Function and Evolution*, Vol. 1, edited by R. SRINIVASAN, pp. 43–57. Oxford: Pergamon Press.

JONES, T. A. (1978). *J. Appl. Cryst.* **11**, 268–272.

KABSCH, W. & SANDER, C. (1983). *Biopolymers*, **22**, 2577–2637.

KIM, H. & LIPSCOMB, W. N. (1991). *Biochemistry*, **30**, 8171–8180.

LIPSCOMB, W. N., COPPOLA, J. C., HARTSUCK, J. A., LUDWIG, M. L., MUIRHEAD, H., SEARL, J. & STEITZ, T. A. (1966). *J. Mol. Biol.* **19**, 423–441.

MANGANI, S. & ORIOLI, P. (1992). *Inorg. Chem.* **31**, 365–368.

READ, R. J. (1986). *Acta Cryst.* A**42**, 140–149.

REES, D. C., LEWIS, M. & LIPSCOMB, W. N. (1983). *J. Mol. Biol.* **168**, 367–387.

SERC Daresbury Laboratory (1979). *CCP4. A Suite of Programs for Protein Crystallography*. SERC Daresbury Laboratory, Warrington, England.